

Mesoscale Modeling of Microstructure Evolution During Thermomechanical Processing

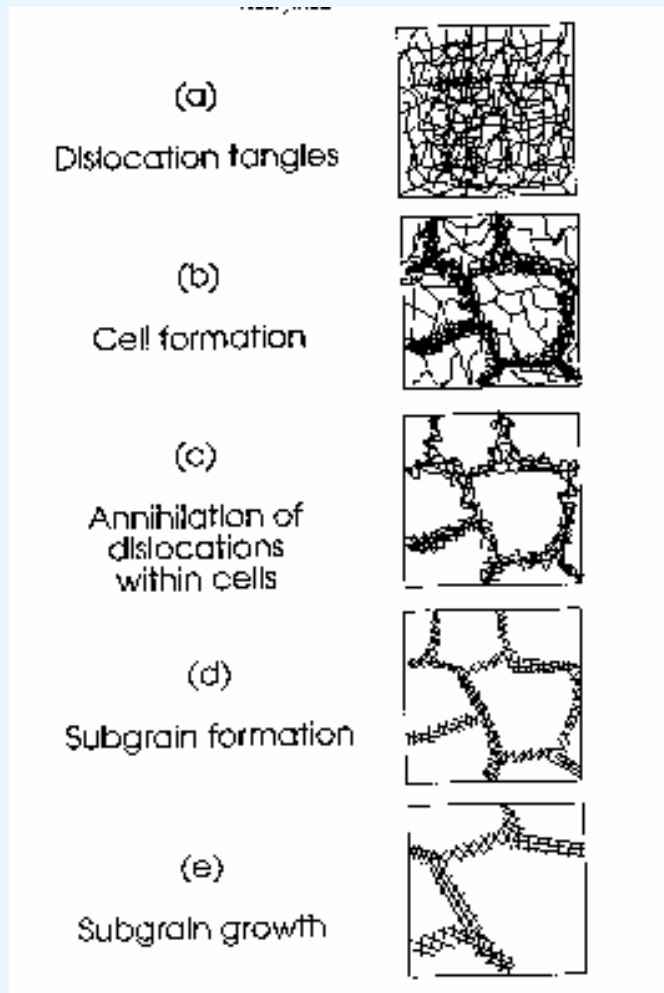
G. Sarma and B. Radhakrishnan

Computer Science and Mathematics Division
Oak Ridge National Laboratory
Oak Ridge, TN 37831-6008

*First ANSWER Workshop
Knoxville, November 16-20, 2003*

**Research Sponsored by the Division of Materials Science and
Engineering, U.S. Department of Energy**

Deformation microstructures contain non-equilibrium defects which evolve during subsequent annealing

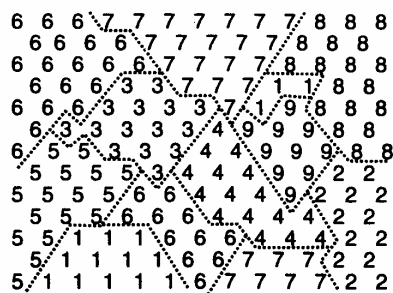
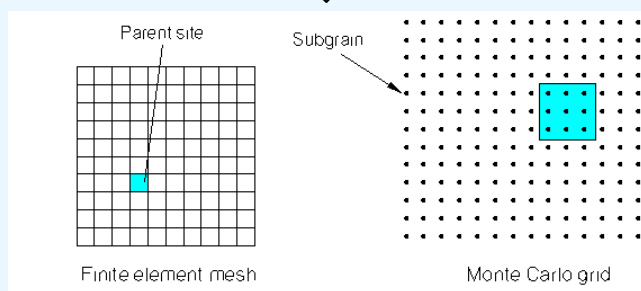
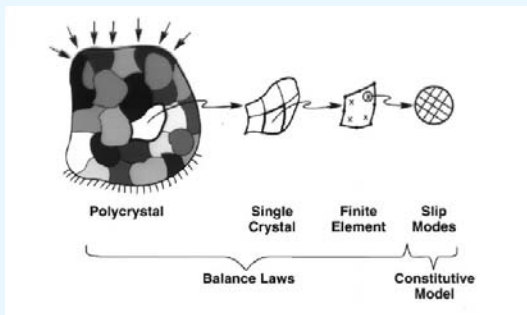


- Deformation substructures consist of
 - dislocations present as subgrain network or tangles
 - excess grain boundary surface area due to grain elongation
- Annealing results in
 - rearrangement and/or elimination of dislocations
 - elimination of stored energy of deformation
 - curvature-driven grain growth

Objective is to develop a fundamental understanding of microstructure evolution during processing

- Dependence of deformation substructure on
 - Initial microstructure
 - Grain size, shape and orientation distribution
 - Second-phase particles
 - Crystal structure
 - FCC, BCC, HCP, poly-phase
 - Stacking fault energy
- Dependence of annealing behavior on
 - Nucleus type and spatial distribution
 - Non-uniform stored energy
 - Orientation gradients
 - Distribution of boundary types, spatial correlation

Coupled Finite Element-Monte Carlo Technique is Used For Modeling the Microstructure Evolution

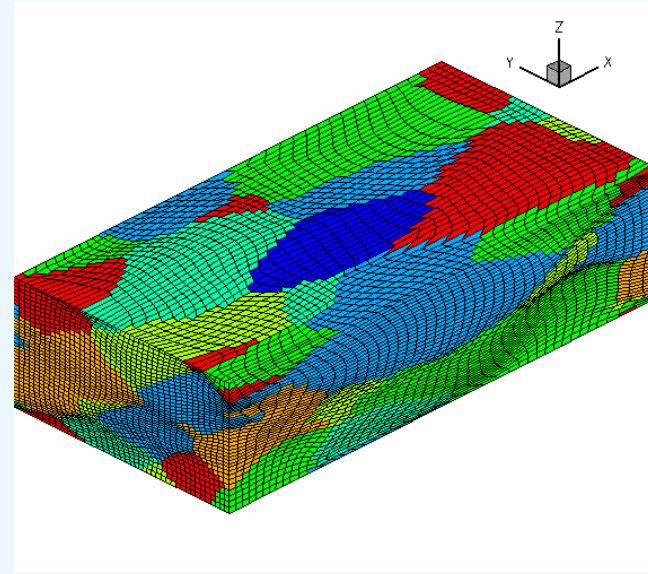
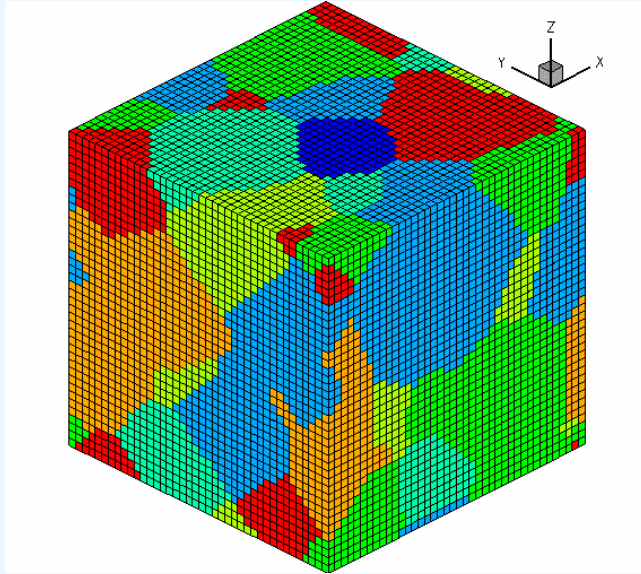


- Microstructural deformation is modeled using FE technique to capture non-uniform stored energy and orientation distributions
- Deformation substructure, assumed to be in the form of well developed subgrain structure, is extracted from FE results

$$H = \frac{\gamma}{2d} \left[\frac{\Delta\theta}{\theta^*} \left(1 - \ln \frac{\Delta\theta}{\theta^*} \right) \right]$$

- Deformation substructure is evolved using a Monte Carlo technique to model kinetics, microstructure and texture after recrystallization

Finite Element Method Coupled With Crystal Plasticity Was Used to Model Deformations at the Mesoscale



- Discretization carried out directly at the grain level to model non-uniform deformations due to grain interactions
- Material constitutive behavior modeled using crystal plasticity to capture anisotropic response and texture evolution
- Formulation implemented on massively parallel computer to enable simulations using large, three-dimensional meshes

Crystal Plasticity Provides the Framework for Modeling Plastic Deformation by Slip

- Power law relates slip system shearing to resolved shear stress
- Schmid orientation tensor is used to relate
 - Crystal deformation rate to slip system shearing rates
 - Crystal stress to slip system resolved shear stress
- Non-linear constitutive relation between stress and deformation rate is solved to obtain the slip system shear rates

$$\tau^\alpha = \tau_{cr} \frac{\dot{\gamma}^\alpha}{\dot{\gamma}_0} \left| \frac{\dot{\gamma}^\alpha}{\dot{\gamma}_0} \right|^{m-1}$$

$$\mathbf{D}_c = \sum_{\alpha} \mathbf{P}^\alpha \dot{\gamma}^\alpha$$

$$\tau^\alpha = \sigma_{ij} n_j^\alpha s_i^\alpha = \boldsymbol{\sigma} \cdot (\mathbf{s}^\alpha \otimes \mathbf{n}^\alpha)$$

$$\mathbf{D}_c = \left[\sum_{\alpha} \left| \frac{\boldsymbol{\sigma} \cdot \mathbf{P}^\alpha}{\tau_{cr}} \right|^{\frac{1}{m}-1} \frac{\dot{\gamma}_0}{\tau_{cr}} \mathbf{P}^\alpha \otimes \mathbf{P}^\alpha \right] \boldsymbol{\sigma}$$

Evolution Laws For Crystal Orientation and Slip System Strength Model Texture and Strain Hardening

- Reorientation of crystal lattice is computed from difference between crystal spin and plastic spin due to slip system shear

$$\dot{\mathbf{R}}^* = \left(\mathbf{W}_c - \sum_{\alpha} \mathbf{Q}^{\alpha} \dot{\gamma}^{\alpha} \right) \mathbf{R}^*$$

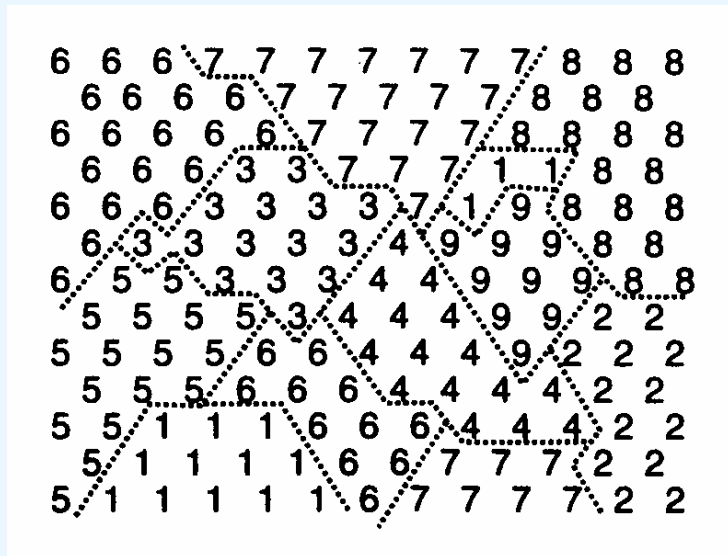
- Strain hardening is modeled through evolution of slip system strength

$$\dot{\tau}_{cr} = H_0 \left(\frac{\tau_{cr}^s - \tau_{cr}}{\tau_{cr}^s - \tau_{cr}^0} \right) \sum_{\beta} |\dot{\gamma}^{\beta}|$$

- Increase in stored energy at each step is proportional to incremental work done at the slip system level

$$\Delta \tau_{cr} \sum_{\beta} |\dot{\gamma}^{\beta}| \Delta t$$

Monte Carlo Simulation of Substructure Evolution – Recrystallization by Abnormal Subgrain Growth



$$E = \frac{1}{2} \sum_i^n \sum_j^{NN} J(S_i S_j) (1 - \delta_{S_i S_j}) \quad N_{MCS}^{\mu\gamma} = N_{MCS} \frac{\mu\gamma}{\mu_{max}\gamma_{max}}$$

$$p(S_i, S_j, \Delta E, T) = \begin{cases} 1 & \Delta E \leq 0 \\ \exp(-\Delta E / kT) & \Delta E > 0 \end{cases}$$

- No bulk stored energy term
- Discretized subgrain structure is represented by orientation numbers
- Each number stands for a crystallographic orientation in the form of an axis-angle pair
- Subgrain boundaries are assumed to exist across sites with unequal numbers
- Grain boundary character is described by misorientation between boundary sites

Grain Boundary Energy and Mobility Depend on the Boundary Misorientation

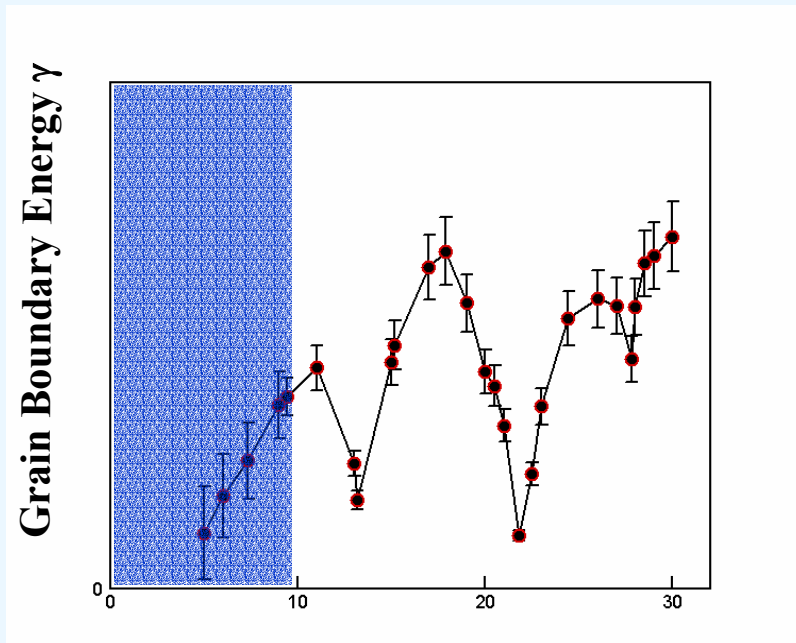
- Boundary energy for general boundaries based on Read-Shockley

$$\gamma = \begin{cases} 0 & \omega = 0 \\ \gamma_0 \frac{\omega}{\omega^*} \left\{ 1 - \ln \left(\frac{\omega}{\omega^*} \right) \right\} & 0 < \omega \leq \omega^* \\ \gamma_0 & \omega > \omega^* \end{cases}$$

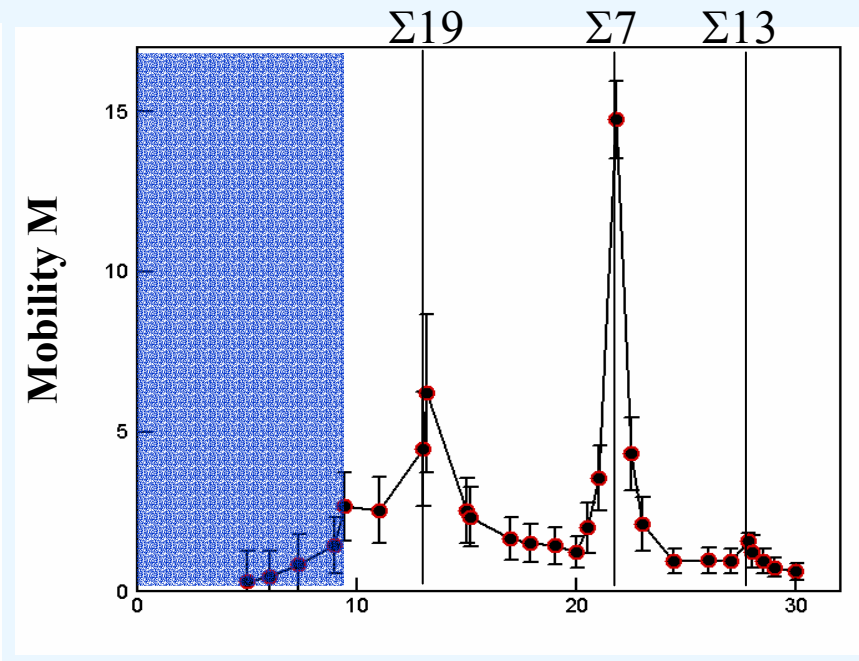
- Boundary mobility for general boundaries based on empirical equation obtained by fitting to experimental data

$$\mu = \mu_0 \left[1 - \exp \left(-k\omega^n \right) \right]$$

Two Different Assumptions Used for Assigning Properties of Special Boundaries



Misorientation θ



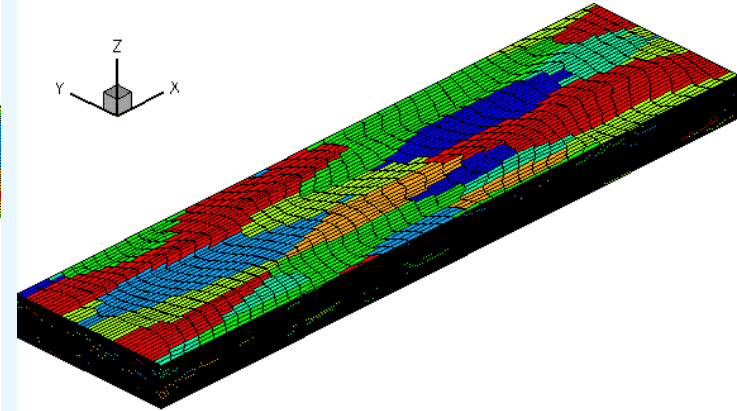
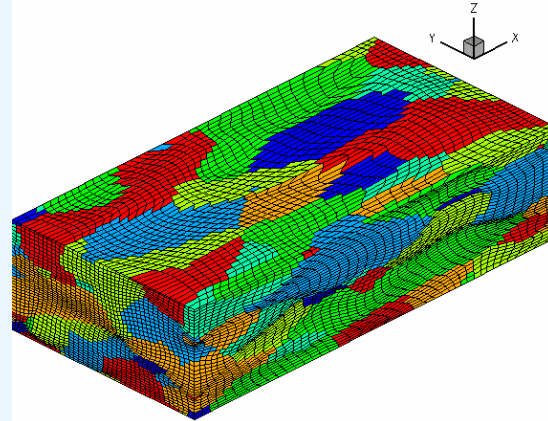
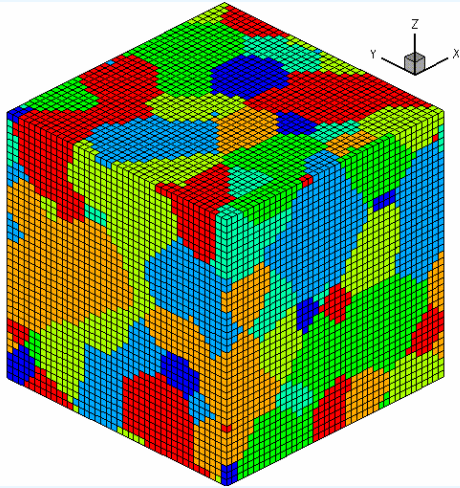
Misorientation θ

- All Σ boundaries ($\Sigma 7$, $\Sigma 13$ and $\Sigma 19$) considered; deviation from Brandon's criterion ($15.0/\Sigma^{-1/2}$) calculated, mobilities and energies assigned by interpolating MD data (from Upmanyu et al.)
- Only $\Sigma 7$ boundaries were considered, and peak mobility and corresponding minimum in energy assigned if Brandon's criterion was satisfied

Mesoscale Model Was Applied to Microstructures Containing Cube, S, and Copper Oriented Grains

- Microstructures were generated using a Monte Carlo grain growth algorithm
- Two microstructures containing 37 and 123 grains in a 40x40x40 grid were chosen
- Grains were randomly assigned orientations from Cube and variants of S ($\{123\}\langle 634\rangle$) and Copper ($\{112\}\langle 111\rangle$)
- Microstructures were also chosen by assigning variants of S or copper orientation, except for a central region of Cube orientation specified as
 - Cube-sphere: spherical region of roughly 10 elements diameter
 - Cube-block: region of size 20x20x10
 - Cube-band: zone of 10 elements thickness along z-axis

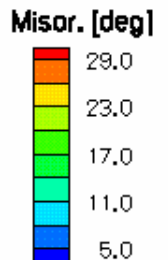
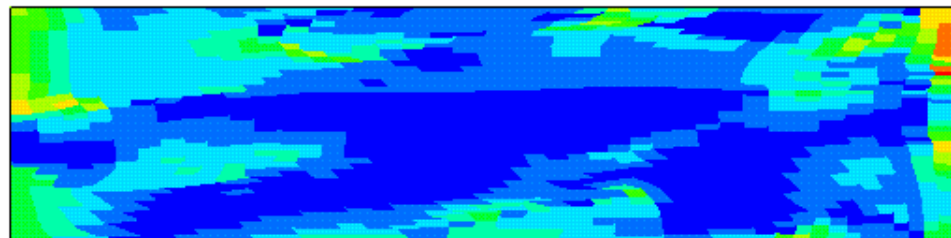
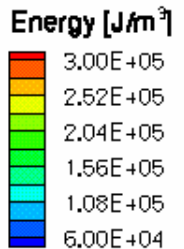
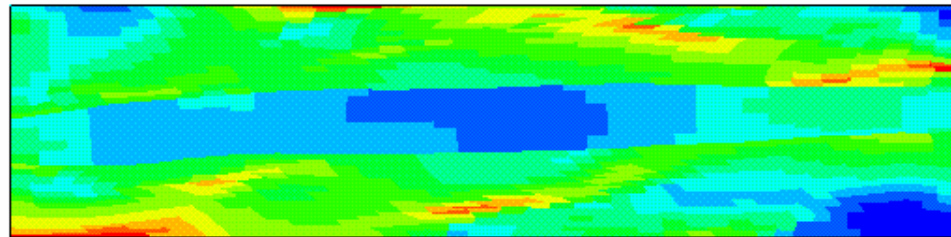
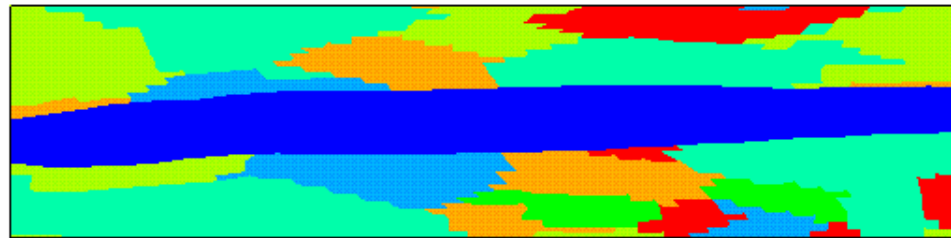
Plane Strain Compression of Microstructures Under Hot Deformation Conditions Were Simulated



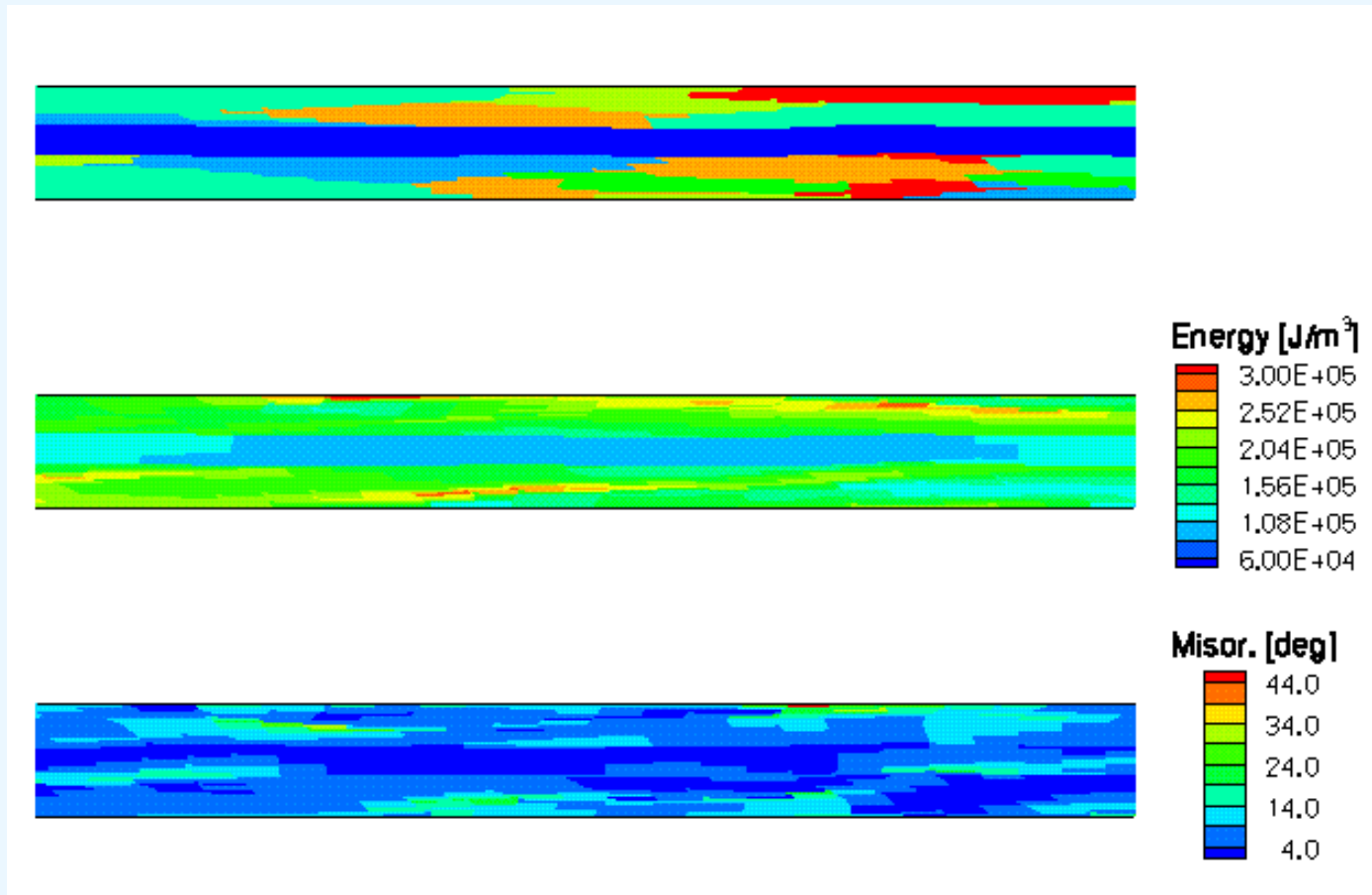
- Material was assumed to have FCC crystal structure
- Material parameters were obtained by fitting compression test data for aluminum deformed at 400°C at various strain rates
- Deformation under elevated temperature conditions was modeled assuming slip on non-octahedral $\{110\}$ planes in addition to $\{111\}$ planes
- Microstructures were deformed in plane strain compression to 50% and 75% reductions in height

Deformation of Microstructure With Band of Cube Orientation After 50% Reduction in Height

- Stored energy is lower in Cube grain and higher in grains above and below
- Misorientation from initial Cube remains low indicating stable deformation
- Regions near the ends of the Cube band are affected by boundary conditions



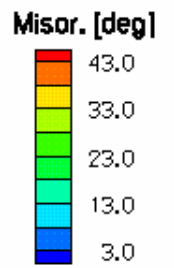
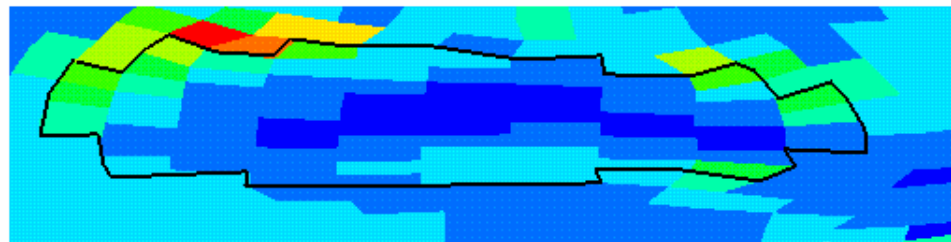
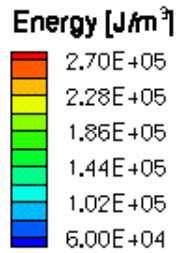
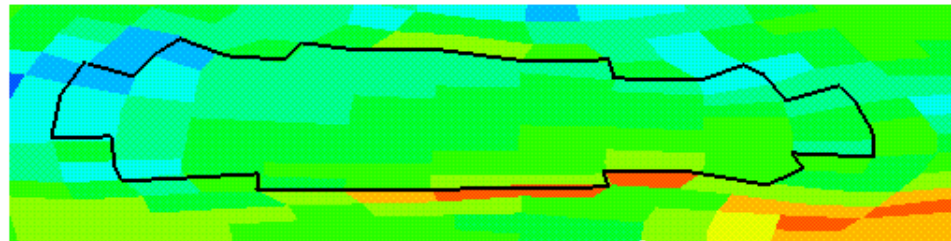
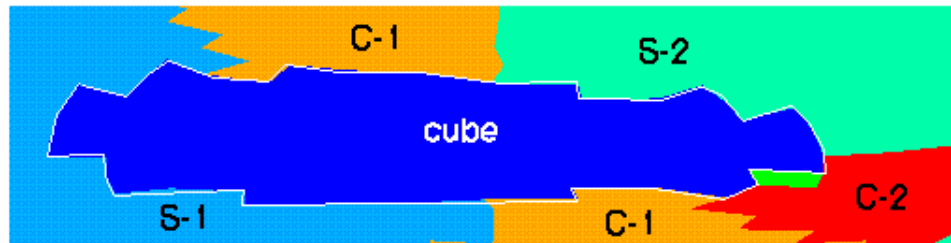
Deformation of Microstructure With Band of Cube Orientation After 75% Reduction in Height



- Overall trends remain similar at higher strain, with lower stored energy and misorientation in Cube grain

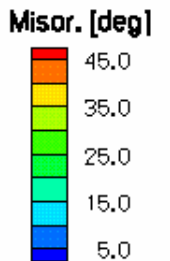
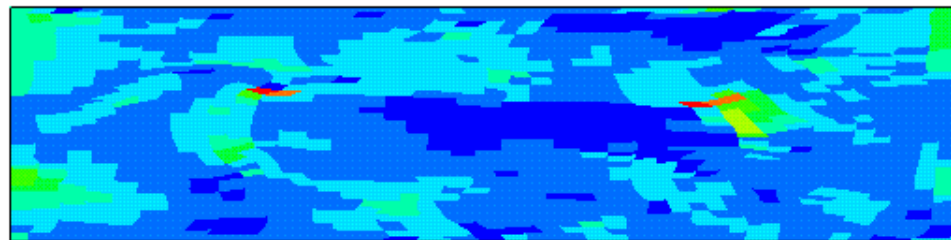
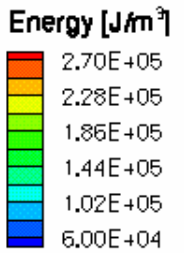
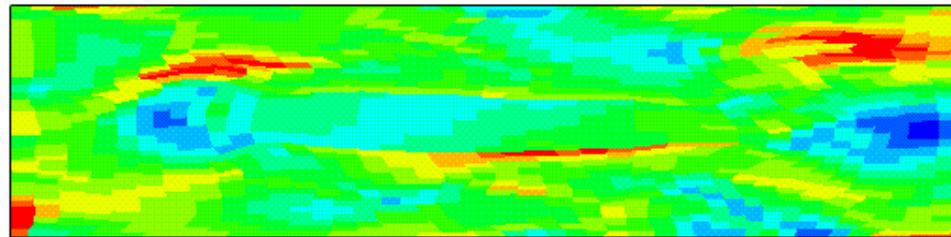
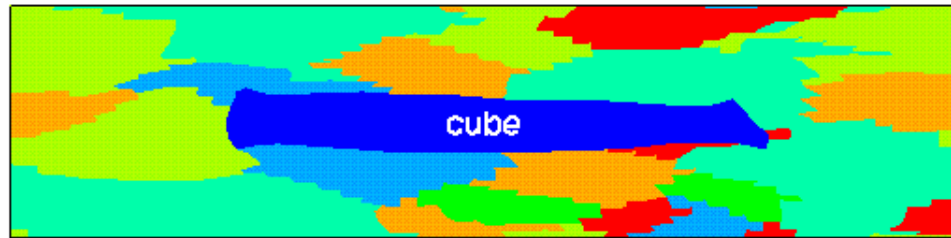
Deformation of Microstructure With Spherical Cube Grain (Mid-section) After 50% Reduction in Height

- Enlarged view shows region around Cube grain
- Stored energy values are higher on the outside of the Cube grain boundary parallel to extension direction
- Deviation from initial Cube is low in the interior and high at the left end of the grain



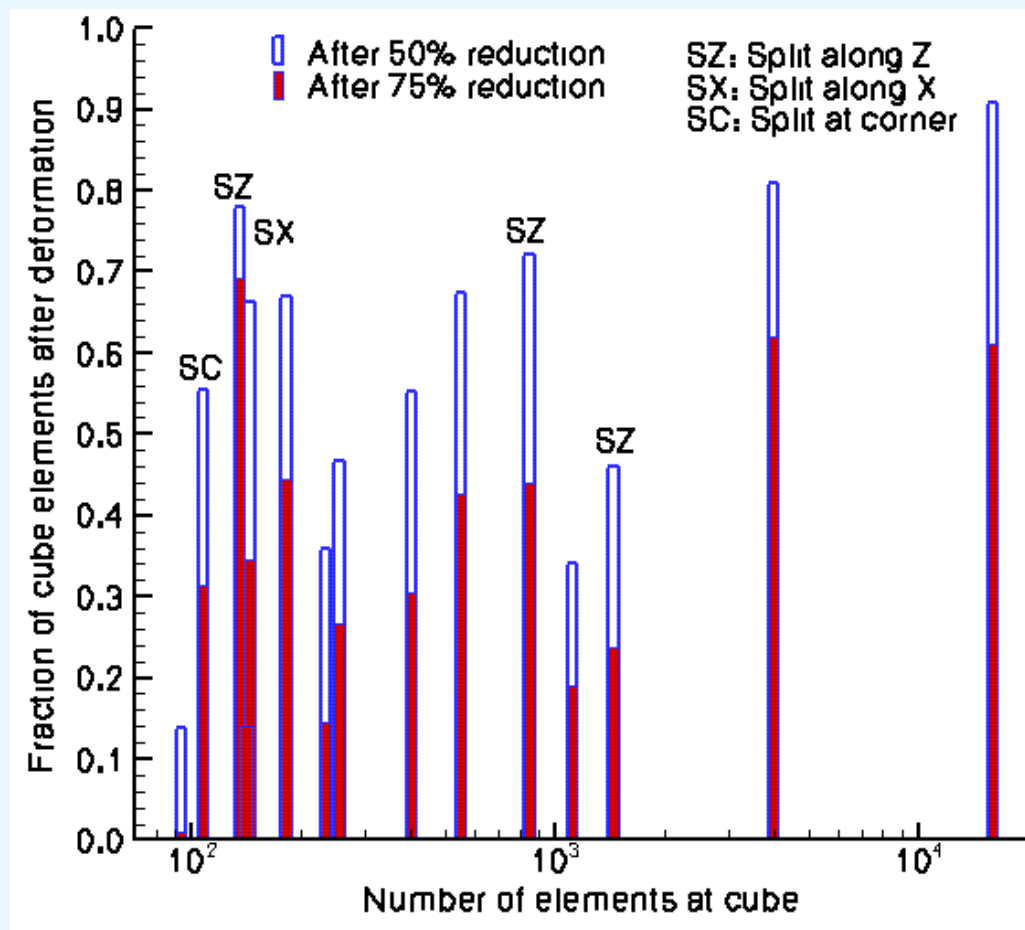
Deformation of Microstructure With Extended Region at Cube Orientation After 50% Reduction in Height

- Band of high stored energy forms immediately adjacent to flat portion of Cube grain boundary
- Stored energy does not change as abruptly across inclined parts of the Cube boundary
- Cube grain retains its orientation except for small sections near inclined boundaries

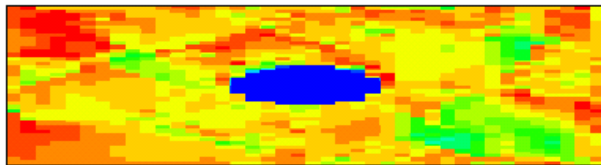
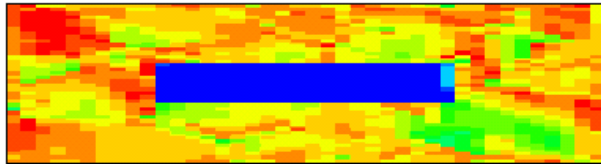
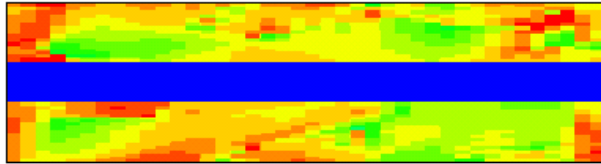


Stability of Cube Grains Depends on Size As Well As Neighborhood

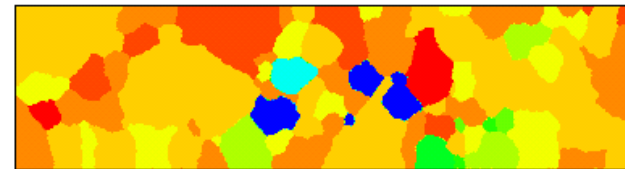
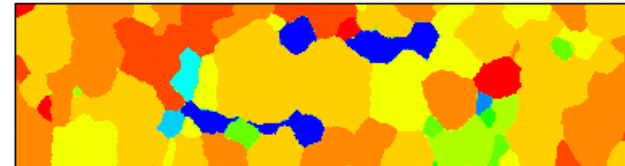
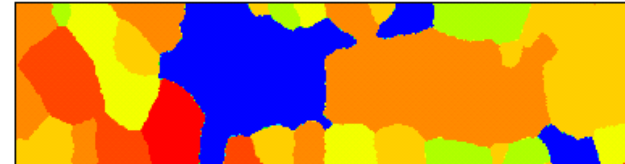
- Overall trend is for Cube grains to be more stable with larger grain size
- Effect of neighborhood is also evident
 - Some small grains remain stable to large strains
 - Some larger grains show greater deviations
- Grains close to surface show influence of boundary constraints
 - Deformation of elements at the surface is closer to ideal plane strain compression



Evolution of Cube Texture During Recrystallization Following 50% Reduction in Height



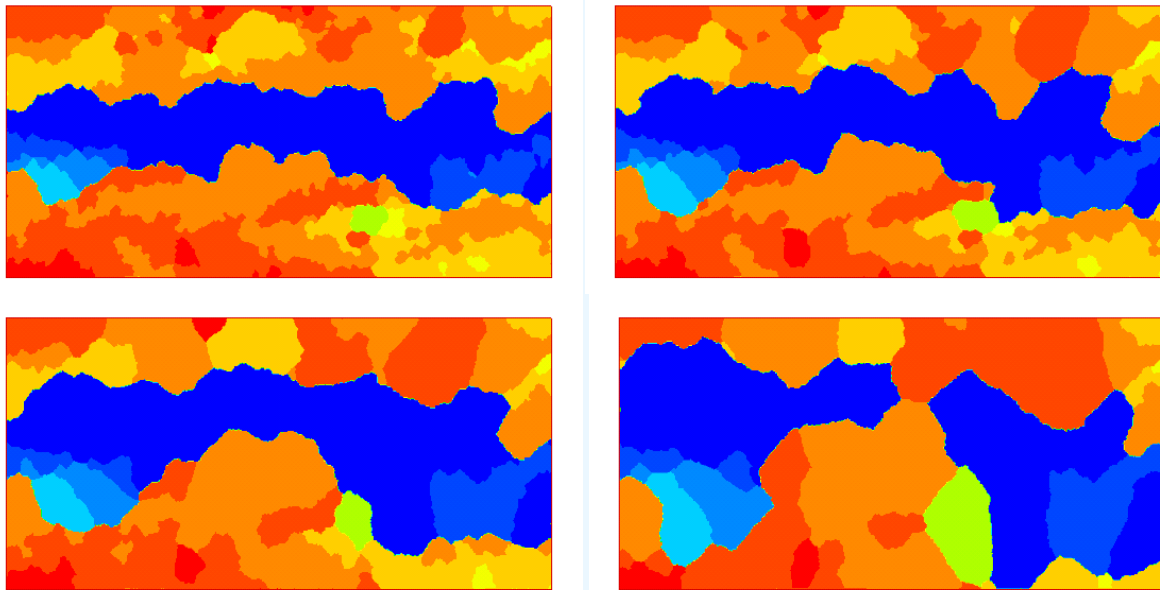
As Deformed



Annealed

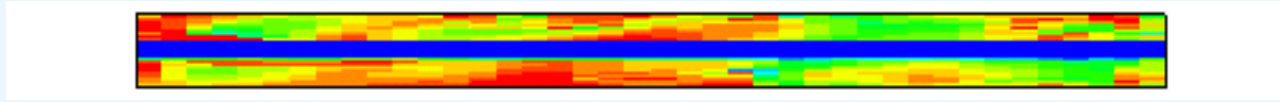
- All special boundaries considered using interpolated boundary energies and mobilities
- Cube grains grow initially to consume non-Cube orientations
- Cube grains are partially consumed by discontinuous growth fronts within non-Cube regions

Evolution of Cube Texture from Cube Band During Recrystallization After 50% Deformation–No End Effects

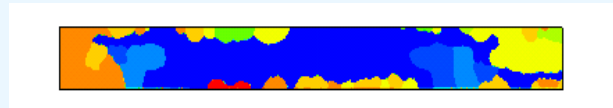


- All special boundaries considered, but no $\Sigma 7$ boundaries adjacent to Cube satisfying Brandon's criterion (deviation $< 7^\circ$) were observed
- Greater volume fraction of Cube compared to the case where end regions were included in simulation
- Discontinuous growth fronts consuming the Cube region are not fully eliminated

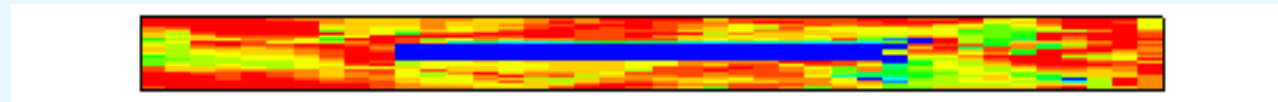
Evolution of Cube Texture from Cube Band After 75% Reduction in Height—No End Effects



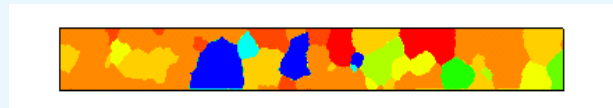
Band



Block



Sphere



- Cube grains in the form of an elongated band contribute to stronger Cube texture after recrystallization

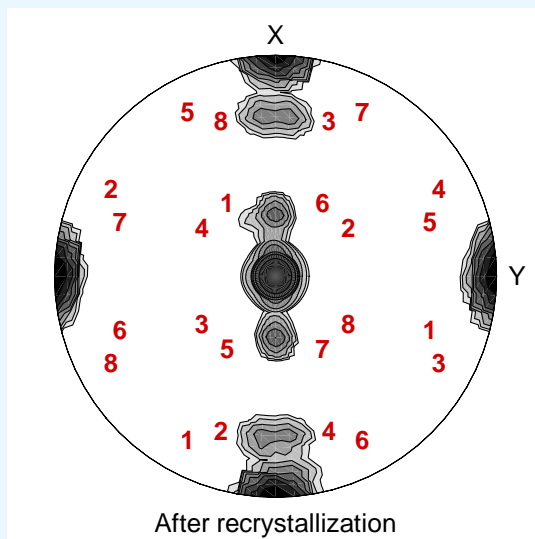
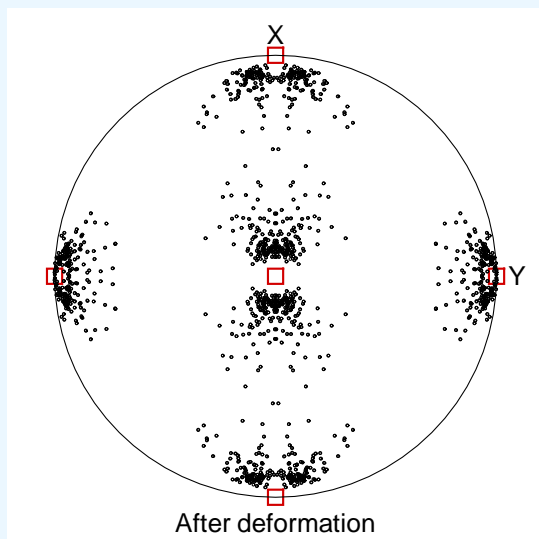
Lower Stored Energy in Cube Grains Leads to Their Growth in Most Cases, but Non-Cube Grains also Grow in Some Cases

- In the S-Cube bicrystal, Cube migrates into S and consumes it during recrystallization; however there are small segments of S that migrate into Cube
- Cube texture evolves by discontinuous evolution of the Cube or near-Cube subgrains by consuming the nearby non-Cube orientations; however, breakaway growth of Cube orientation does not occur because of the presence of discontinuous growth fronts in non-Cube regions
 - local differences in the stored energy of deformation between the Cube and non-Cube regions can lead to discontinuous growth fronts in the non-Cube regions
- The substructure evolution appears to be quite sensitive to the choice of the boundary properties used for special boundaries
 - correct choice of subgrain properties should be based on experimental observations of the occurrence of special boundaries
- End-constraints in finite element simulations appear to have influenced the simulation results

Coupled Mesoscale Model Was Applied to Single Crystals and Bi-crystals With and Without Particles

- Single crystals of different orientations, and with different shapes for hard particles were modeled
 - Cube (001)[100], S (123)[6 3 4], and Copper (112)[1 1 1]
 - Spherical, cube and rotated cube particles
- Bi-crystals with and without a spherical hard particle at the grain boundary were modeled
 - S-Cube, S-Copper, and Copper-Cube bi-crystals
- Hard particle was modeled by setting the slip system strength of associated elements above the saturation value
- Plane strain compression under hot deformation conditions was simulated to 40% reduction in height

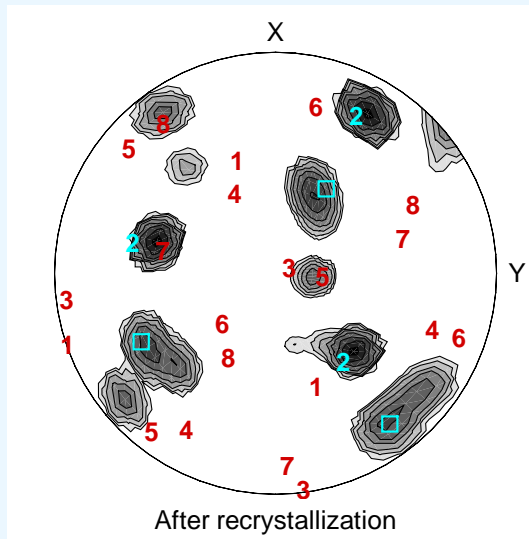
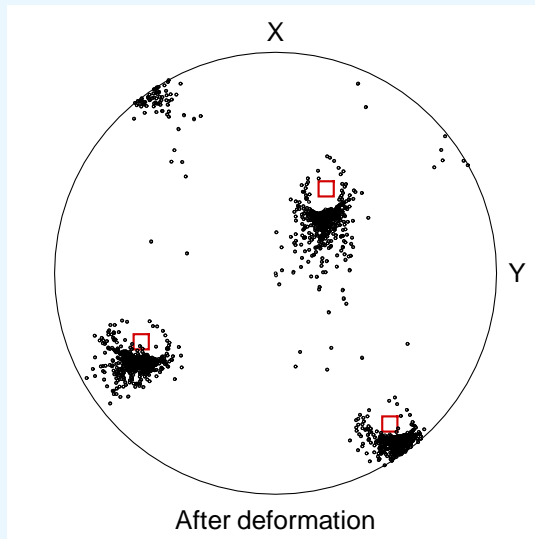
Cube Oriented Grain with Hard Particle Shows Some TD Rotated Components After Recrystallization



Number	Rotation axis
1	111
2	<u>1</u> 11
3	1 <u>1</u> 1
4	11 <u>1</u>
5	<u>1</u> <u>1</u> 1
6	<u>1</u> 1 <u>1</u>
7	<u>1</u> <u>1</u> <u>1</u>
8	<u>1</u> <u>1</u> <u>1</u>

- Only elements that are misoriented by more than 5° from Cube (deformation zone) are shown in deformation texture
- Recrystallized texture does not coincide with any of the $40^\circ \langle 111 \rangle$ rotations of Cube

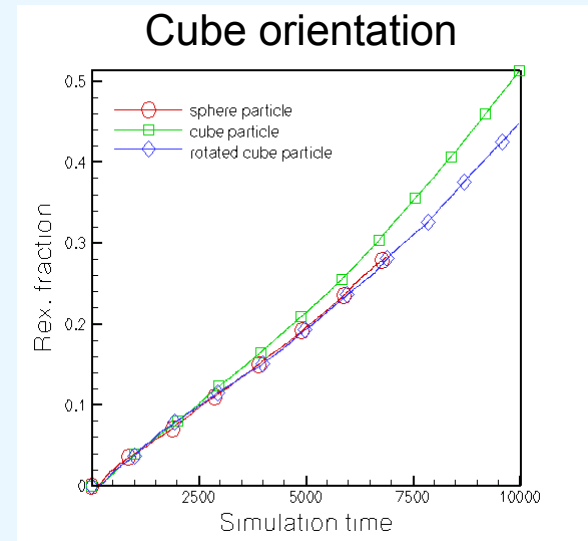
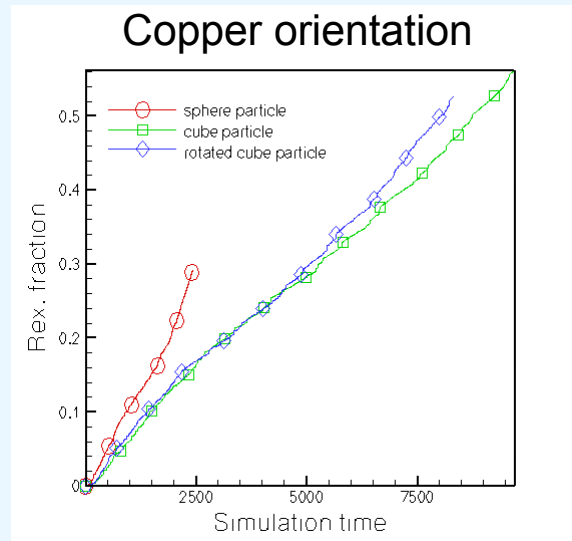
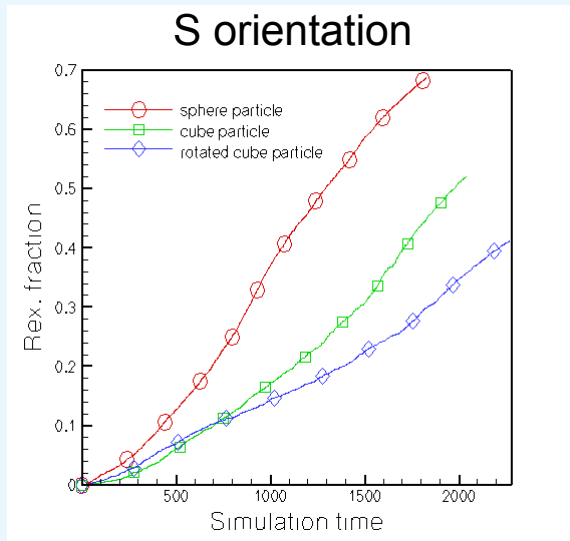
S Oriented Grain with Spherical Hard Particle Shows Strong $40^\circ\langle 111 \rangle$ Recrystallization Texture



Number	Rotation axis
1	111
2	$\underline{1}11$
3	$1\underline{1}1$
4	$11\underline{1}$
5	$11\underline{1}$
6	$\underline{1}1\underline{1}$
7	$\underline{1}11$
8	$11\underline{1}$

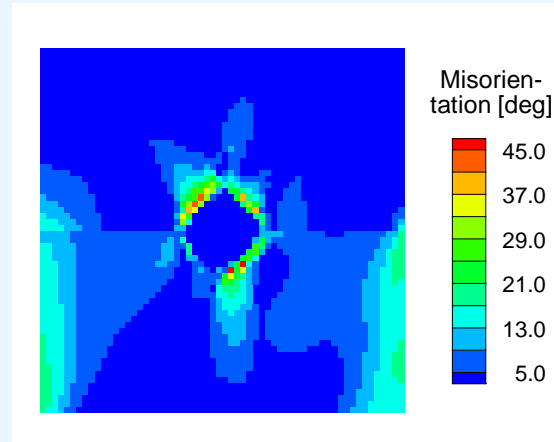
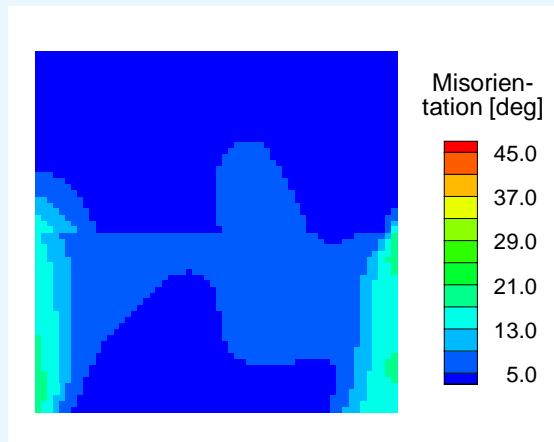
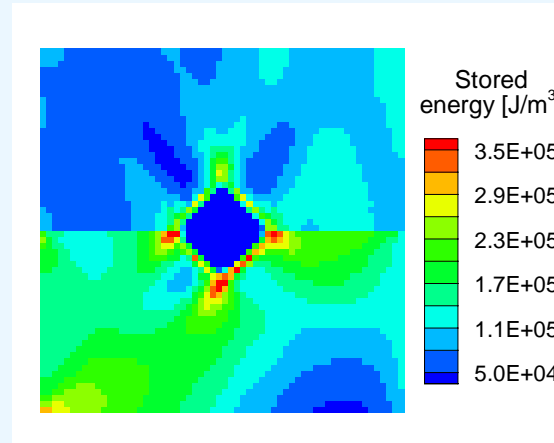
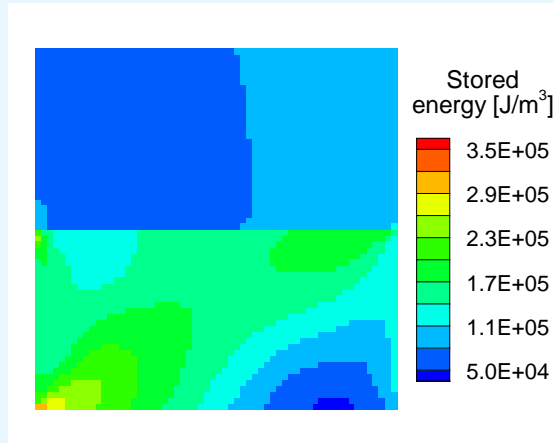
- Only elements deviated by more than 5° from S (deformation zone) are shown after deformation
- Significant increase in intensity of an orientation very close to $40^\circ[\underline{1}11]$ rotation of S is observed
- Rex. texture also includes weaker “random” components not misoriented by $40^\circ\langle 111 \rangle$ from S

Effect of Particle Shape and Initial Orientation are Seen in the Recrystallization Kinetics



- All particle shapes produced nuclei with special $40^\circ \langle 111 \rangle$ misorientation for the S oriented crystal, leading to faster kinetics
- Only spherical particle produced specially oriented nuclei for the crystal initially at Copper orientation
- None of the particle shapes produced specially oriented nuclei for the crystal initially at Cube orientation

Stored Energy and Misorientation Distributions For S-Cube Bi-crystal With and Without Spherical Hard Particle

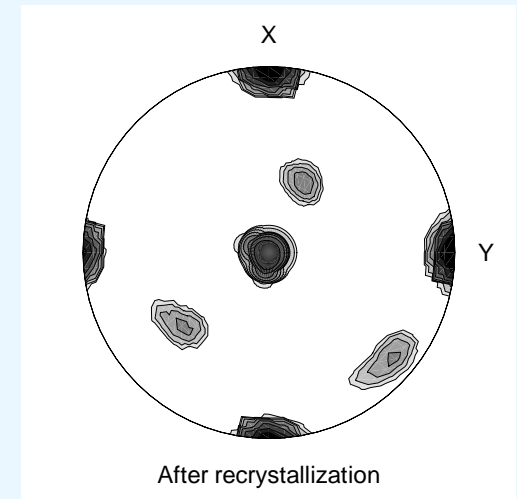
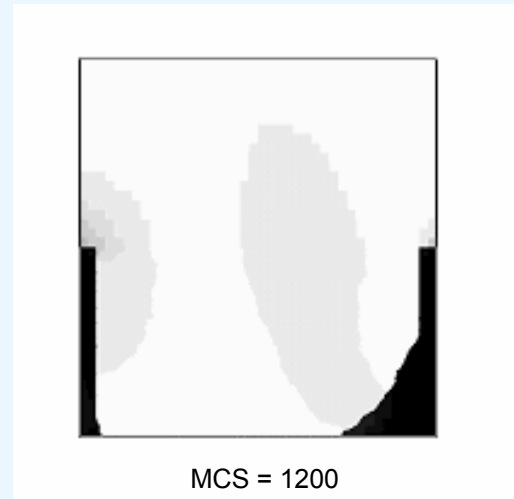
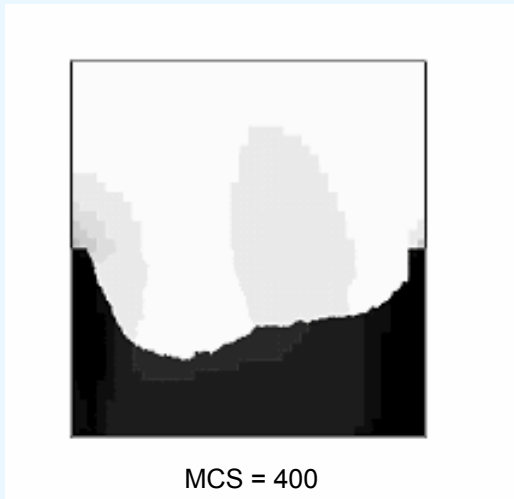


Without particle

With particle

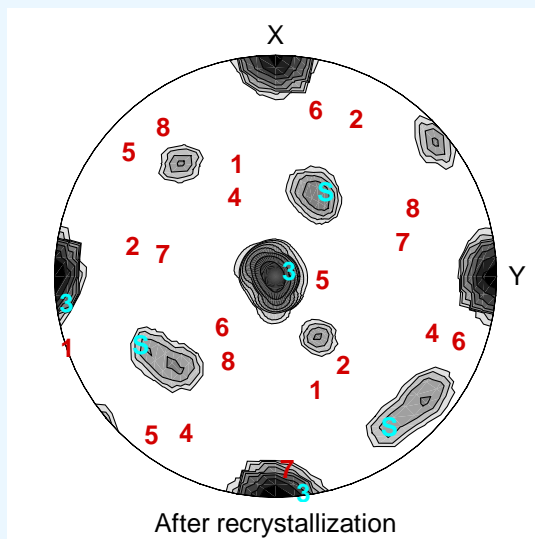
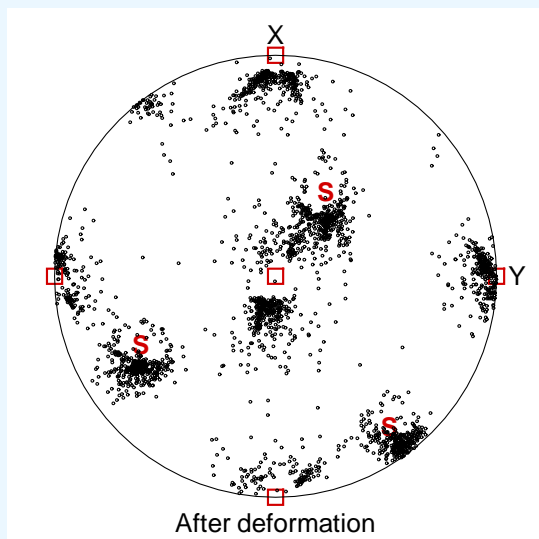
- Stored energy is lower in Cube grain compared to S
- Stored energy is higher in the deformation zone close to the particle
 - Stored energy is higher on S side near the particle
- Misorientation from the initial orientation is much higher in the vicinity of the particle

S-Cube Bi-crystal Shows Strong Cube Texture After Recrystallization



- Lower stored energy on Cube side causes growth of Cube grain into S by strain induced boundary migration (SIBM)
- Growth of cube grain is aided by special $40^\circ\langle 111 \rangle$ misorientation between Cube and S

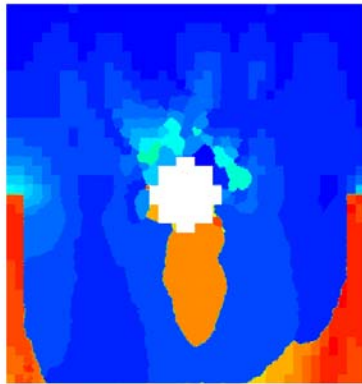
S-Cube Bi-crystal with Hard Particle Shows Strong Cube Texture After Recrystallization



Number	Rotation axis
1	$1\bar{1}1$
2	$\bar{1}11$
3	$1\bar{1}1$
4	$1\bar{1}\bar{1}$
5	$\bar{1}\bar{1}1$
6	$\bar{1}\bar{1}\bar{1}$
7	$\bar{1}\bar{1}1$
8	$1\bar{1}\bar{1}$

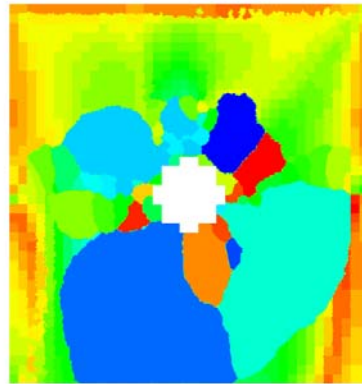
- Recrystallized texture has a strong $40^\circ[1\bar{1}1]$ rotation of S
 - Corresponds to misorientation between Cube and S (migration of interface)
- Particle stimulated nucleation contributes weaker “random” components

Hard Particle at Bi-crystal Boundary can have Significant Effect Depending on Grain Orientations



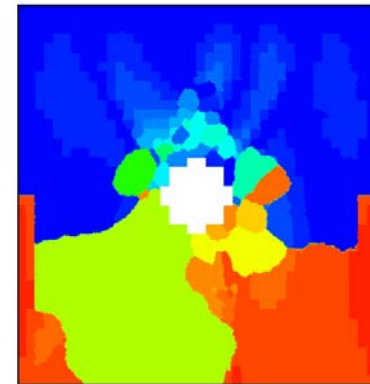
MCS = 1200

Cube-S



MCS = 1200

Copper-S

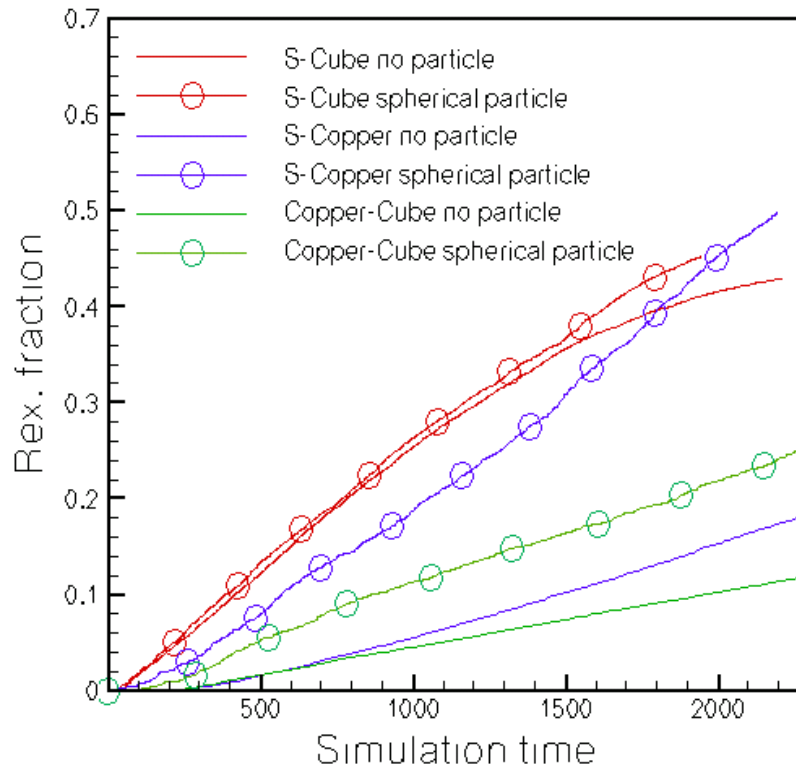


MCS = 1200

Cube-Copper

- No significant effect due to particle for S-Cube bi-crystal
 - Nucleus produced in the S grain is overtaken by migration of Cube-S interface
- Significant effect for Copper-S and Cube-Copper bi-crystals
 - Special nuclei form in S grain for Copper-S bi-crystal and in Copper grain for Cube-Copper bi-crystal

Recrystallization Kinetics of Bi-crystals is Enhanced Significantly in the Presence of Particles



- Cube-Copper and S-Copper bi-crystals containing particles recrystallize faster than particle-free bi-crystals
- No significant effect for the S-Cube bi-crystal since the PSN nuclei are quickly consumed by the migrating S-Cube interface
- Recrystallization kinetics of S-Cube bi-crystal without particle is faster than other bi-crystals with particles
 - S-Cube interface is a special boundary with a near $40^\circ \langle 111 \rangle$ misorientation with S

Summary and Conclusions

- Deformation simulations captured the formation of localized deformation zones near particles situated inside single crystals, bicrystal boundaries and triple line of a tricrystal
- The recrystallization texture is dominated by the growth of nuclei that are rotated by $40^\circ\langle 111 \rangle$ in some instances, while in others such orientations were absent
- There were also weaker, “random” orientations that were far from the special orientations
- The formation of the special $40^\circ\langle 111 \rangle$ nuclei appeared to depend on the initial matrix orientation as well as the particle shape
- Formation of special boundaries in the particle deformation zone also led to increase in the recrystallization kinetics compared to the particle-free case

Acknowledgments

- Research sponsored by the Division of Materials Science and Engineering, U.S. Department of Energy, under contract DE-AC05-00OR22725 with UT-Battelle, LLC.
- This research used resources of the Center for Computational Sciences at Oak Ridge National Laboratory, which is supported by the Office of Science of the U.S. Department of Energy, under contract DE-AC05-00OR22725.
- The submitted manuscript has been authored by a contractor of the U.S. Government under contract No. DE-AC05-00OR22725. Accordingly, the U.S. Government retains a non-exclusive, royalty-free license to publish or reproduce the published form of this contribution, or allow others to do so, for U.S. Government purposes.